

- no, Jr., T. T. Conrad, and G. A. Tharp, *J. Am. Chem. Soc.*, 1982, **104**, 4429.
11. A. Mori and H. Takeshida, *Bull. Chem. Soc. Jpn.*, **58**(5), 1581 (1985).
12. Sung Sik Kim, Dong Yeol Yoo, In Ho Cho, and Sang

- Chul Shim, *Bull. Korean Chem. Soc.*, **8**(4), 296 (1987).
13. Sung Sik Kim, Dong Yeol Yoo, and In Ho Cho, *Bull. Korean Chem. Soc.*, **9**(4), 257 (1988).
14. Sung Sik Kim, Yong Joon Yoon, In Ho Cho, and Sang Chul Shim, *Bull. Korean Chem. Soc.*, **8**(5), 429 (1987).

Lone Pairs in the 1,3-Sigmatropic Group Rearrangements¹

Ikchoon Lee*, Jeoung Ki Cho, and Bon-Su Lee

Department of Chemistry, Inha University, Incheon 402-751

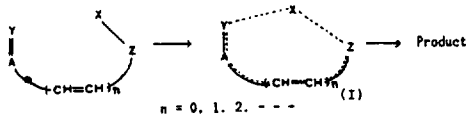
Hyuck Keun Oh

Department of Chemistry, Chonbuk National University, Chonju 560-756. Received August 31, 1988

Semiempirical computations using the AM1 and MNDO methods were carried out in order to elucidate allowed mechanisms for 1,3-group(X) rearrangement processes with X = BH₂, CH₃, CN, F, NH₂, OH, Cl and SH. The reactivity of the group migration was largely controlled by the steric effect in the 4-membered ring transition state, an antarafacial process having a greater energy barrier due to a greater steric repulsion. For the groups with lone pair electrons, the participation of the lone pair orbital is found to ease the steric effect by enabling the FMO interaction with highly polarizable, high lying, lone pair electrons at relatively distant range; the involvement of lone pairs in the transition state causes an alteration of the symmetry selection rule to that of a 6-electron system with an allowed 1,3-suprafacial migration in contrast to an allowed 1,3-antarafacial migration for a 4-electron system. Various stereoelectronic aspects were analysed in some detail.

Introduction

In a sigmatropic rearrangement, an atom or a group migrates from one end of a conjugated π system to the other through a cyclic transition state (TS), I, (Scheme 1).² In our previous papers, various types of sigmatropic hydrogen rear-



Scheme 1

rangements have been reported; Y and Z in scheme 1 have been varied to give 1,3- and 1,5-(Y, Z)-H shifts³ and the system with A = nitrogen has also been dealt with⁴.

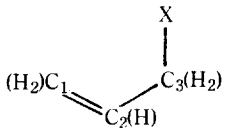
In this work, we report the results of our semiempirical MO studies on the group(X) migration in propene, X-CH₂-CH=CH₂ with X = CH₃, BH₂, NH₂, OH, CN, F, Cl, and SH; by examining frontier MO(FMO) patterns⁵, symmetry rules⁶, and electronic charge shifts, we attempted to explain the reactivity trend in this work. We made special reference to the change of symmetry rules for the groups with lone pairs for which the TS (I) becomes a 6-electron system and the 1,3-sigmatropic retentive migration involves a suprafacial process in contrast to an allowed 1,3-antarafacial process in the 4-electron system.

Calculation

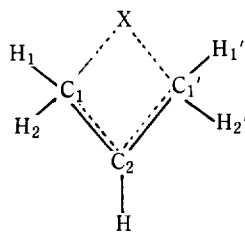
Computations were performed using the AM1^{7,8} and MNDO^{7,9} methods. Geometries of the ground state (GS) and

the TS were fully optimized by the method of gradient norm minimization¹⁰; whenever applicable, symmetry elements were introduced in the optimization of the TS structure. In the force constant matrix calculations¹¹ for the TS characterization, three cases were found to arise: (i) zero negative eigenvalue; for the 6-electron migration, with X = F and NH₂, a shallow minimum is obtained so that no negative eigenvalue appeared. For this type of behavior, McIver *et al.*, reported that the TS has a symmetric structure¹², the energy difference between the minimum and the TS being 0.5–1.0 kcal/mol with a rapid energy drop near the products (or reactants). The PMO analysis of Dewar *et al.*¹³ have shown that pericyclic reactions are continuous, and synchronous processes, but the shallow minimum found in the Cope rearrangement had energy difference which is well within the computational error¹⁴. On the other hand, such shallow minimum obtained with a low level ab initio calculations turned out to be a maximum (TS) when a full CI calculations were carried out¹⁵. (ii) One negative eigenvalue; this is the normal case for the TS in the symmetry allowed processes. (iii) Two negative eigenvalues; when a migration group (X) with lone pairs was forced to be located within the molecular plane in an antarafacial migration, which was considered only for the comparison with the allowed suprafacial process, two negative eigenvalues appeared, one for the stretching and the other for the out-of plane bending modes of the C-X bond. However for X = NH₂, one negative eigenvalue was obtained for the antarafacial process, since zero negative eigenvalue was found for the suprafacial TS.

For the GS, the most stable, *s-cis*, conformers only were considered, since these are the crowded forms of heavy atom

Table 1. Geometries of the Ground States (Bond Lengths and Angles are in Å and Degrees Respectively.)


X	Parameter	C ₁ C ₂	C ₂ C ₃	C ₃ X	C ₁ C ₂ C ₃	C ₂ C ₃ X
AM1	CH ₃	1.3305	1.4821	1.5071	126.01	114.76
	NH ₂	1.3296	1.4961	1.4392	126.11	118.81
	OH	1.3296	1.4854	1.4155	127.57	117.82
	CN	1.3300	1.4855	1.4465	125.68	114.39
MNDO	BH ₂	1.3411	1.4995	1.5464	129.24	116.32
	CH ₃	1.3399	1.5031	1.5298	129.92	118.61
	NH ₂	1.3396	1.5103	1.4641	130.34	119.54
	OH	1.3397	1.5101	1.3960	129.78	112.65
	CN	1.3402	1.5046	1.4572	129.30	116.80
	F	1.3395	1.5170	1.3524	129.26	115.15
	Cl	1.3399	1.4947	1.8070	129.93	115.54
	SH	1.3402	1.4988	1.7293	129.40	115.32

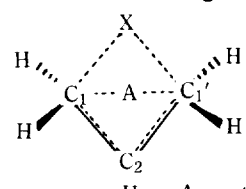
Table 2. Geometries of the Antarafacial Transition State (Bond Lengths and Angles are in Å and Degrees Respectively.)


X	Parameter	C ₁ C ₂	C ₁ X	C ₂ X	C ₁ C ₁ '	C ₁ 'XC ₁ H ₁	C ₁ 'XC ₁ H ₂
AM1	NH ₂	1.4598	1.5437	2.0796	2.1653	120.38	-120.38
	OH	1.4389	1.6846	2.0730	2.3199	117.71	-117.71
	CN	1.4441	1.6507	2.1935	2.1735	126.41	-114.71
MNDO	BH ₂	1.4887	1.6324	2.1370	2.2695	114.39	-114.39
	NH ₂	1.4570	1.5634	2.0810	2.1863	121.60	-121.60
	OH	1.4647	1.5025	2.0218	2.1714	121.68	-121.68
	CN	1.4580	1.6259	2.1701	2.1846	124.63	-116.19
	F	1.4695	1.4977	2.0509	2.1441	121.81	-121.81
	Cl	1.4335	2.0194	2.4537	2.3592	122.33	-122.33
	SH	1.4507	1.8504	2.2487	2.3783	120.76	-120.76

skeleton which are present prior to the reaction. Some TS structures were not obtainable due to the convergency problems. The structures determined are summarized in Tables 1-3.

Results and Discussion

FMO theory provides a simple yet a powerful and versatile method of explaining the pattern of reactivity in pericyclic reactions. We will make ample use of the HOMO-LUMO interactions⁵ schemes in discussing various aspects of reactivity.

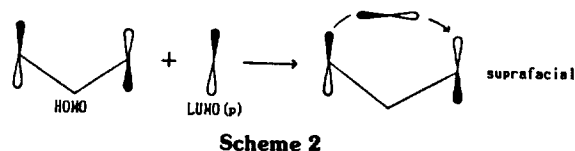
Table 3. Geometries of the Suprafacial Transition State (Bond Lengths and Angles are in Å and Degrees Respectively.)


X	Parameter	C ₁ C ₂	C ₁ X	C ₂ X	C ₁ C ₁ '	AC ₂ N	AC ₂ H ₁
AM1	R-CH ₃ ^a	1.4022	2.1517	2.5892	2.2226	24.14	161.12
	I-CH ₃ ^b	1.3843	2.4083	2.5162	2.4257	43.20	164.42
	NH ₂	1.4532	1.5734	2.0758	2.1601	12.23	161.93
	OH	1.4176	1.7868	2.1004	2.2754	24.66	155.76
	CN	1.3902	2.2694	2.5794	2.2943	32.00	160.92
MNDO	BH ₂	1.4537	1.6987	1.8105	2.4236	31.10	158.33
	R-CH ₃ ^a	1.4227	1.8587	2.4380	2.1296	11.21	168.50
	I-CH ₃ ^b	1.3872	2.9300	2.9523	2.4728	56.40	173.46
	NH ₂	1.4528	1.5871	2.0792	2.1833	10.87	166.61
	OH	1.4559	1.5410	2.0493	2.1567	10.31	164.17
	Cl	1.4114	2.1963	2.4890	2.3608	29.17	160.48
	SH	1.4380	1.9026	2.2517	2.3228	22.88	160.82

^a R: retention, ^b I: inversion.

A. MO Patterns. We summarize various MO patterns involved in the allowed 1,3-group (X) migrations based on the results of our AM1 and MNDO calculations.

X = CH₃. The FMO pattern for the TS can be constructed using the HOMO of propenyl fragment and the LUMO of the CH₃ group. When CH₃ interacts in the migration as a σ -type orbital, the allowed process is an antarafacial type, which incurs however prohibitively large steric effect. As a result, a suprafacial p-type migration becomes an allowed process (Scheme 2).



X = BH₂. Since the atom B is small and has a low lying vacant p orbital, the HOMO-LUMO interaction, which is of the same type suprafacial migration, becomes allowed.

X = CN. The C atom in this group can interact either as a σ -LUMO or as a p-HOMO, since π electron in the group can participate in the migration (Scheme 3).

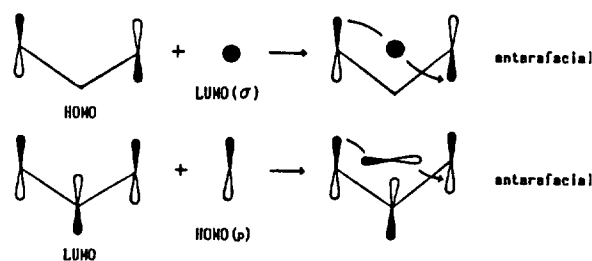
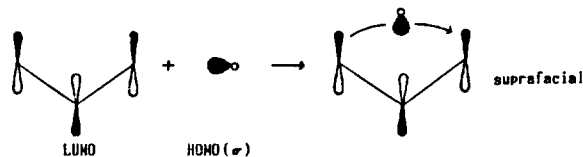


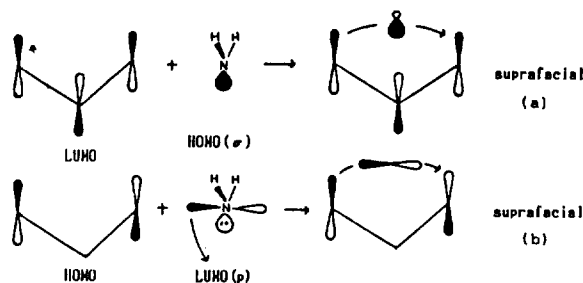
Table 4. The HOMO Energy Level (eV) of σ -Lone Pair on the Group X

	NH ₂	OH	F	Cl	SH
AM1	-12.006	-13.021			
MNDO	-12.646	-12.670	-16.022	-13.266	-9.846

X = OH, Cl, SH: The heteroatoms are relatively large and have high lying lone pair (n) orbitals. The LUMO of the propenyl system interacts with the HOMO of X in a suprafacial process (scheme 4).

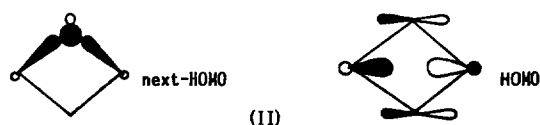
**Scheme 4**

X = NH₂. Due to the two H atoms, σ -HOMO and p-LUMO of N atom interact with LUMO and HOMO of the propenyl system respectively in suprafacial processes. The former type belongs to the same category as the groups with high lying lone pairs above (Scheme 4). In Scheme 5, the MOs

**Scheme 5**

formed by the interaction of propenyl and NH₂ fragments, a and b, are the next HOMO and HOMO of the TS respectively.

X = F. The lone pair on F has very low energy and is small sized compared with that on other atoms so that the system forms a planar TS¹⁶, (II). Comparisons of calculated

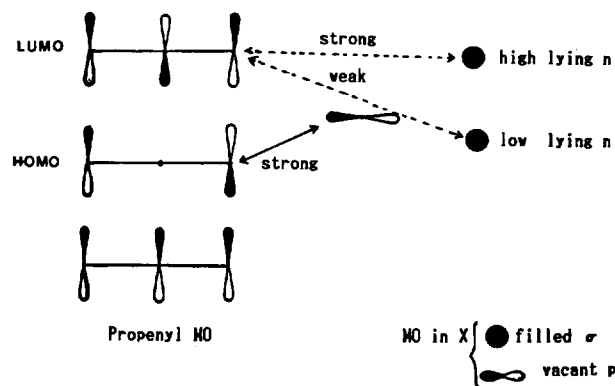
**(II)**

lone pair energies are shown in Table 4. Due to the exceptionally low lying lone pair (n) level in F, the LUMO(propenyl system)-HOMO(n on F) interaction will have insignificant contribution (Scheme 6) to the TS involved in the migration, while a high lying lone pair (n) orbitals in other groups i.e., Cl, SH, etc will interact efficiently with the propenyl LUMO as shown in Scheme 6. This is the reason why the participation of lone pair electrons in the group migrations with the high lying n levels is possible and the selection rule is altered to that for 6-electron system.

B. 4-Electron vs 6-Electron Process. Since the lone pair, n, level in the migrating group constitutes the HOMO, the X will be an electron-donor in the 6-electron system, whereas the X will become an electron-acceptor in the 4-electron

Table 5. Electron Density Variation Patterns along the Reaction Coordinate

X	AM1				MNDO			
	C ₁	C ₂	C ₃	X	C ₁	C ₂	C ₃	X
BH ₂	↗	↘	↗	↘	↗	↘	↗	↘
CH ₃	↗	↘	↗	↘	↗	↘	↗	↘
CN	↗	↘	↗	↘	↗	↘	↗	↘
NH ₂	↗	↘	↗	↘	↗	↘	↗	↘
OH	↗	↘	↗	↘	↗	↘	↗	↘
F	↗	↘	↗	↘	↗	↘	↗	↘
Cl	↗	↘	↗	↘	↗	↘	↗	↘
SH	↗	↘	↗	↘	↗	↘	↗	↘

**Scheme 6**

system in which the LUMO of X interacts with the HOMO of the propenyl system, Scheme 7. In the case of X = CN, an

**Scheme 7**

electron-acceptor being a typical 4-electron system, the overall electron shift appears to be very small due to the contribution of π electrons as an electron-donor, Scheme 8.

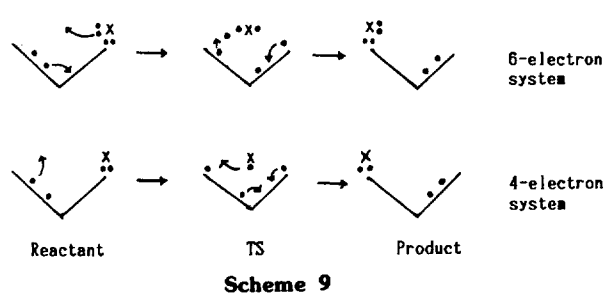
**Scheme 8**

The electron density variations along the reaction coordinate¹⁷ for each migrating group are shown schematically in Table 5. Reference to this table indicates that the trends exhibited by the two systems, i.e., 4- and 6-electron systems, are in general opposite; as expected from the electron flows in Scheme 7 and 8, electron density at C₂ (X) increases (decreases) in the 6-electron systems while it decreases (increases) or shows little variation in the 4-electron systems. These changes are consistent with the formal participation of 6-electrons or 4-electrons in the actual rearrangements as shown in Scheme 9.

Two exceptions are found in the electron density variation: X = OH by AM1 and X = Cl and SH by MNDO for which the electron density in X are continuous or return to

Table 6. Activation Enthalpies, ΔH^\ddagger , and Energy Component for Activation Processes in 1,3-Sigmatropic Rearrangements
(A: antarafacial, S: suprafacial)

Component X	H^\ddagger (kcal/mol)		$(V_{nn} - V_{ee})^\ddagger$ (eV)		$2\Delta\Sigma\epsilon_i^\ddagger$ (eV)		
	A	S	A	S	A	S	
AM1	CH ₃	130.95 ^a	106.51 ^b	-7.1319 ^a	-7.0953 ^b	12.8103 ^a	11.7142 ^b
	NH ₂	80.10	75.57	4.0997	-0.6665	-0.6263	3.9437
	OH	155.56	78.51	-21.6520	-16.1909	28.3977	19.5955
	CN	102.25	116.28	-7.0289	15.7810	11.4630	20.8234
MNDO	BH ₂	43.82	24.13	2.8055	9.2749	-1.0043	-8.3284
	CH ₃	138.36 ^a	123.37 ^b	-1.4174 ^a	-8.6703 ^b	7.4173 ^a	14.0199 ^b
	NH ₂	61.16	59.01	3.2722	-0.4139	-0.6202	2.9727
	OH	89.65	82.42	8.2497	6.7793	-4.3621	-3.2053
	CN	91.93		-5.7969		9.7836	
	F	102.79		15.1106		-10.6529	
	Cl	80.09	56.15	-0.0172	-7.3608	3.4903	9.7956
	SH	88.78	57.53	-2.9139	-2.4102	6.7634	4.9048

^a retention, ^b inversion.

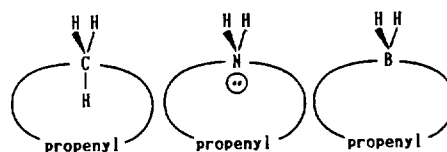
the original value. This can be rationalized by an abnormal electron localization behaviour on oxygen found with AM1 and by the possible involvement of d orbitals in the 3rd row element as well as the good leaving ability of Cl. An initial increase of electron density at C₃ is due to the π electron shift accompanying the attack by lone pairs, and after some progress along reaction coordinate the density on C₃ decreases due to the scission of C₃-X bond. For X = CN, the electron density of C₂ and X in the GS and TS appears to be similar even though the density on each atom actually varies as the reaction progresses from the GS to the TS.

C. Reactivity. Energy components, one-electron ($2\Delta\Sigma\epsilon_i^\ddagger$) and steric ($\Delta(V_{nn} - V_{ee}^\ddagger)$) terms¹⁸, are summarized together with activation enthalpies in Table 6 for various systems. The reactivity is found to decrease in the order, X = BH₂ > Cl, SH > NH₂ > OH > CN > F > CH₃, demonstrating that in general the activation barriers are lower with the systems which proceed by the sterically favorable suprafacial process. The BH₂ group has the most efficient HOMO-LUMO interaction¹⁹ giving the lowest energy barrier, since it can utilize a low lying empty p-orbital in addition to its small size. In contrast, the systems with high lying lone pair orbitals (Cl and SH) can also achieve an efficient FMO interaction at relatively distant position in the four-membered ring TS, despite the substantial steric repulsion between the lone pair and the propenyl π system due to the relatively large size.

For the small sized F which has the extremely low energy lone pair orbital, the activation barrier is very high. This is partly due to the less efficient FMO interaction of lone pair

orbital (scheme 6) which forces this group to behave as a 4-electron system, and the antarafacial process (4-electron, allowed) becomes competitive with the suprafacial one (6-electron, allowed). This why the X group is located within the molecular plane, (II), rendering high steric repulsion. The CH₃ group has the highest barrier since the three H atoms sterically interact within 4-membered TS, although the migration takes place suprafacially. In contrast, the CN group has somewhat lower barrier than the CH₃ group due to an extra stabilizing interaction of C \equiv N π orbitals in addition to the lack of sterically unfavorable H atoms.

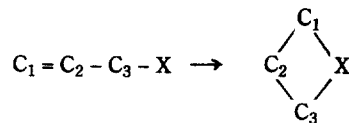
Some of the Factors Relevant to the Reactivity are. (i) Retention vs inversion. The TS structures in scheme 10 are 5-coordinated and similar to those of bimolecular nucleophilic



reactions, so that the inversion products will be obtained with the p-type migration of the CH₃, NH₂, and BH₂ groups. Although theoretical calculations using the MINDO/3, INDO, and STO-3G methods have been reported to predict retention for such type of migration²⁰, experimental investigations on very similar systems using optical activities have shown that the process occurs with inversion²¹.

(ii) Steric effect. As the 4-membered ring TS is formed in the course of reaction, bond angle and orbital distortions become excessive resulting in a greater steric inhibition. Thus the large sized migrating groups with high lying lone pairs can minimize the steric effect by utilizing the lone pairs in the migration (6-electron system) to enable an efficient, long range FMO interactions. In this respect, a long range polarization of electrons with the 3rd row element, Cl and SH, will help to avoid closer approach in reducing steric repulsion.

(iii) Electron density. Charge dispersion in the TS will lower orbital energies so that lower activation barrier will be obtained. This means that charge localization is to be avoid-

Table 7. Electron Density (in Electron Unit) Variation Patterns along the Reaction Coordinate

X	Parameter	AM1				MNDO			
		C ₁	C ₂	C ₃	X	C ₁	C ₂	C ₃	X
BH ₂	GS					-0.0640	-0.1001	-0.0381	0.1551
	A					-0.1309	0.4276	-0.1309	-0.3285
	S					-0.0605	0.1551	-0.0605	-0.3141
CH ₃	GS	-0.2258	-0.1603	-0.1339	-0.2105	-0.0558	-0.1130	0.0195	0.0297
	R-TS	0.2416	-0.5981	0.2416	-0.6732	0.4205	-0.7343	0.4205	-0.3193
	I-TS	-0.2206	-0.1582	-0.2206	-0.2586	-0.0824	-0.0847	-0.0824	-0.0479
NH ₂	GS	-0.2290	-0.1994	-0.0634	-0.3349	-0.0546	-0.1511	0.1197	-0.2774
	A	0.1154	-0.8256	0.1154	-0.1113	0.3133	-0.7731	0.3133	-0.1117
	S	0.0576	-0.6467	0.0576	-0.1588	0.2660	-0.6453	0.2660	-0.1429
OH	GS	-0.2206	-0.1953	0.0035	-0.3311	-0.0215	-0.1354	0.2045	-0.3257
	A	-0.4693	0.4443	-0.4693	-0.2514	0.4121	-0.7949	0.4121	-0.2763
	S	0.0682	-0.3323	0.0682	-0.4544	0.3180	-0.6430	0.3180	-0.2199
CN	GS	-0.1992	-0.1758	-0.0464	-0.1390	-0.0300	-0.1356	0.1447	-0.1053
	A	-0.1470	-0.1296	-0.1470	-0.1355	0.0373	-0.0995	0.0373	-0.1175
	S	0.2597	-0.4158	0.2597	-0.6027				
F	GS					-0.0149	-0.1747	0.2689	-0.2439
	A					0.4011	-0.8094	0.4011	-0.0908
Cl	GS					-0.0089	-0.1605	0.1709	-0.2189
	A					0.5079	-0.8524	0.5079	-0.2550
	S					0.3183	-0.3639	0.3183	-0.5273
SH	GS					-0.0308	-0.1204	-0.0436	0.0518
	A					0.3936	-0.8279	-0.3936	-0.0942
	S					0.1437	-0.4249	0.1437	0.0774

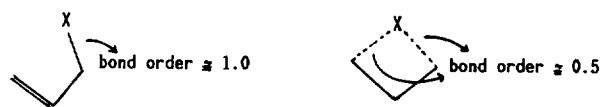
R-TS: retention-TS, I-Ts; inversion-TS, A; anatarafacial, S; suprafacial.

Table 8. Bond Order for the Bond Between X and a Terminal Carbon in the TS

Process X	AM1		MNDO	
	antarafacial	suprafacial	antarafacial	suprafacial
BH ₂			0.8991	0.7336
CH ₃	0.2923 ^a	0.5019 ^b	0.4528 ^a	0.4983 ^b
CN	0.6395	0.0968	0.6588	
NH ₂	0.8538	0.7594	0.8135	0.7444
OH	0.5581	0.5024	0.7102	0.6892
F			0.6817	
Cl			0.5781	0.3545
SH			0.7148	0.6593

^a retention, ^b inversion.

11).

**Scheme 11**

Inspection of Table 8 reveals that the bond order of the C-X bond in the TS for the suprafacial inversion process of the CH₃ group is indeed about 0.5, whereas the migrating groups with high lying lone pairs show considerably greater bond order than 0.5, correctly reflecting the involvement of lone pairs in the TS formation. For X = OH with AM1 and X = Cl with MNDO, however, the bond orders are abnormally low, indicating again the weakness of AM1 for overlocalizing electronic charges on O atom and exceptionally good leaving ability of Cl, besides the high electronegativities of the two atoms. For X = CN, the bond order is also high because of π electron participation in the TS formation. This is evident from little variation of core electron density (AM1, $C_{-0.1390} \equiv N_{-0.0496}(\text{GS}) \rightarrow C_{-0.1355} \equiv N_{-0.1500}(\text{TS})$; MNDO, $C_{-0.1053} \equiv N_{-0.0826}(\text{GS}) \rightarrow C_{-0.1175} \equiv N_{-0.1559}(\text{TS})$) accompanied by a large variation in bond order (AM1, $\text{GS}_{2.9062} \rightarrow \text{TS}_{2.5934}$; MNDO, $\text{GS}_{2.9202} \rightarrow \text{TS}_{2.5631}$) as the reaction proceeds from

ed in order to achieve a greater TS stabilization. Table 7 shows that suprafacial processes are more favorable in this respect than antarafacial processes allowing a greater degree of charge dispersion within the TS structure.

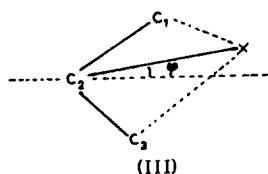
(iv) Bond order. Since the bond order of the C-X bond is approximately 1.0 in the GS, the sum of bond orders of the two C-X bonds in the TS should also be ~ 1.0 , provided the C-X bond alone participates in the TS formation²² (Scheme

Table 9. The Angle (ϕ in Degree) Obtained from the Optimized TS Geometries

System	X	AM1	MNDO	Type of process and remarks
4-electron	CN	0.00	0.00	σ -antarafacial, no σ -lone pair no hydrogen
system	BH ₂	31.10	10.87	p -suprafacial, most effective HOMO-LUMO interaction
	CH ₃	43.20	56.40	p -suprafacial three hydrogen atom
6-electron	F	0.00	0.00	σ -antarafacial, extremely low HOMO level, small lone-pair
system	OH	24.66	10.31	σ -suprafacial, moderate size lone-pair
	NH ₂	12.23	10.87	p -suprafacial, moderate size lone-pair
	SH	22.88	22.88	σ -suprafacial, 3rd period atom large size lone-pair
	Cl	29.17	29.17	σ -suprafacial, 3rd period atom large size lone-pair

the GS to the TS; the partial breaking of C \equiv N π bonds will enable the π electrons to participate in the TS formation. For BH₂, a large amount of electron flow into a vacant p orbital shows up in a greater increase in the bond order.

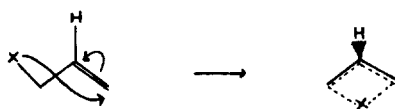
D. Structures. The angle ϕ (III), between C₂-X and the



propenyl molecular plane in the TS differs depending of the group X. The angle (ϕ) obtained from the optimized TS geometries are shown in Table 9.

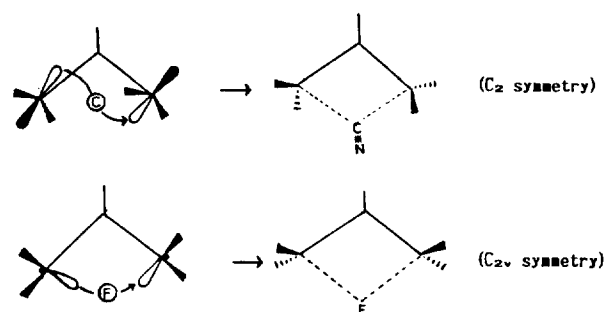
The BH₂ group is the smallest with a vacant p orbital so that the most efficient FMO interaction is to be expected on steric ground; this system may therefore be considered to give an optimum angle with $\phi = 31.10^\circ$. With the 3rd row elements, Cl and SH, this angle is approximately maintained because of their long range polarization of lone pairs giving low steric effect. With X = CH₃ the angle increases to 56.40° and the FMO interaction decreases considerably.

In the suprafacial processes, the H atom on the central carbon also deflects toward the migrating group and deviates from coplanarity (Scheme 12). The migrating group CN and

**Scheme 12**

F have near zero ϕ ²³ with two different TS symmetries of C₂ and C_{2v}, respectively (Scheme 13), since both migrate antarafacially but CN has π type interaction while F migrates with a σ -type interaction.

In summary, we have seen that in the 1,3-sigmatropic group rearrangements, large steric inhibition is inevitable because of the 4-membered ring type TS formation; as a result the use of a large group with highly polarizable lone pair may cause deviation from coplanarity but can maintain

**Scheme 13**

an efficient attractive orbital interaction.

Acknowledgement. We thank the Ministry of Education and the Korea Science and Engineering Foundation for support of this work.

References

- Determination of Reactivity by MO Theory, part 57.
- (a) R. C. Bingham and M. J. S. Dewar, *J. Am. Chem. Soc.*, **94**, 9107 (1972); (b) S. Kato and K. Fukui, *ibid.*, **99**, 684 (1977); (c) W. J. Bouma, D. Poppinger, and L. Radom, *ibid.*, **99**, 6443 (1977); (d) W. J. Bouma, and L. Radom, *ibid.*, **101**, 3487 (1979); (e) L. Carlsen and F. Duus, *ibid.*, **100**, 281 (1978); (f) A. D. Isaacson and K. Morokuma, *ibid.*, **97**, 4453 (1975); (g) J. E. Del Bene and W. L. Kochenour, *ibid.*, **98**, 2041 (1976); (h) P. D. Adeney, W. J. Bouma, L. Radom, and W. R. Rodwell, *ibid.*, **102**, 4069 (1980); (i) W. J. Bouma, M. A. Vincent, and L. Radom, *Int. J. Quantum Chem.*, **14**, 767 (1978); (j) W. R. Rodwell, W. J. Bouma, and L. Radom, *ibid.*, **18**, 107 (1980); (k) K. Yamashita, H. Kaminoyama, T. Yamabe, and K. Fukui, *Theor. Chim. Acta.*, **60**, 302 (1981).
- J. K. Cho, I. Lee, and H. K. Oh, and I. H. Cho, *J. Korean Chem. Soc.*, **28**, 217 (1984).
- J. K. Cho, I. Lee, H. K. Oh, and I. H. Cho, *Bull. Korean Chem. Soc.*, **5**, 179 (1984).
- (a) R. B. Woodward and R. Hoffmann, *Angew. Chem. Int. Ed. Engl.*, **8**, 781 (1969); (b) M. J. S. Dewar, *ibid.*, **10**, 761 (1971); (c) K. Fukui, "Theory of Orientation and Stereoselection," Berlin and New York, Springer-Verlag, 1975; (d) K. Fukui, *Acc. Chem. Res.*, **4**, 57 (1971); (e) I. Fleming, "Frontier Orbitals and Organic Chemical Reactions," New York, John Wiley and Sons, 1976.
- (a) R. B. Woodward and R. Hoffmann, "The Conservation of Orbital Symmetry," Berlin, Verlag Chemie GmbH, 1971; (b) R. G. Pearson, "Symmetry Rules for Chemical Reactions," New York, John Wiley and Sons, 1976; (c) T. L. Gilchrist and R. C. Storr, "Organic Reactions and Orbital Symmetry," 2nd ed., Cambridge University Press, Cambridge, 1979.
- M. J. S. Dewar, E. G. Zoebisch, E. F. Healy, and J. J. P. Stewart, *J. Am. Chem. Soc.*, **107**, 3902 (1985).
- Available from Quantum Chemistry Program Exchange (QCPE), No. 506.
- M. J. S. Dewar and W. J. Thiel, *J. Am. Chem. Soc.*, **99**, 4899 (1977).
- A. Komornichi, K. Ishida, and K. Morokuma, *Chem. Phys. Lett.*, **45**, 595 (1979).
- J. W. McIver, Jr. and A. Komornichi, *J. Am. Chem. Soc.*,

- 94**, 2625 (1972).
12. R. E. Stanton and J. W. McIver, Jr. *J. Am. Chem. Soc.*, **97**, 3632 (1975).
 13. M. J. S. Dewar and R. C. Dougherty, "The PMO Theory of Organic Chemistry," Plenum Press, New York, 1975.
 14. M. J. S. Dewar and C. Jie, *J. Am. Chem. Soc.*, **109**, 5893 (1987).
 15. C. Doubleday, Jr. R. N. Camp, H. F. King, J. W. McIver, Jr. D. Mullally, and M. Page, *J. Am. Chem. Soc.*, **106**, 447 (1984).
 16. For this, ab initio computations (3-21G, 6-31G, and 6-31G*) have shown that the migration takes place suprafacially; Unpublished result.
 17. (a) K. Muller, *Angew. Chem. Int. Ed., Engl.* **19**, 1 (1980); (b) S. Bell and J. S. Crighton, *J. Chem. Phys.*, **80**, 2464 (1984).
 18. M. J. S. Dewar, "The MO Theory of Organic Chemistry," McGraw-Hill, New York, 1969.
 19. (a) F. Bernardi, A. Mangini, N. D. Epiotis, J. R. Larson, and S. Shaik, *J. Am. Chem. Soc.*, **99**, 7465 (1977); (b) F. Bernardi, A. Bottoni, and N. D. Epiotis, *ibid.*, **100**, 7205 (1978).
 20. N. D. Epiotis, R. L. Yates, and F. Bernardi, *J. Am. Chem. Soc.*, **97**, 4198 (1975).
 21. (a) J. Slutsky and H. Kwart, *J. Am. Chem. Soc.*, **95**, 8678 (1973); (b) J.A. Berson and G.L. Nelson, *J. Am. Chem. Soc.*, **89**, 5303 (1967); (c) J.A. Berson, *Acc. Chem. Res.*, **1**, 152 (1968).
 22. H. S. Johnston and C. Parr, *J. Am. Chem. Soc.*, **85**, 2544 (1963).
 23. In the Process from reactant to TS, CN or F did not migrate along the CCC plane.

Photoaddition Reactions of *p*-Quinones to Conjugated Diyne

Sung Sik Kim*, Dong Yeol Yoo, Ae Rhan Kim, and In Ho Cho

Department of Chemistry, Chonbuk National University, Chonju 560-756

Sang Chul Shim

Department of Chemistry, Korea Advanced Institute of Science and Technology, Seoul 131-650

Received September 5, 1988

Irradiation of solutions of *p*-quinones and conjugated diyne, 1,4-diphenylbutadiyne, with 350 nm UV light gave the photoproducts such as quinomethane in good yields (70-85%).

Introduction

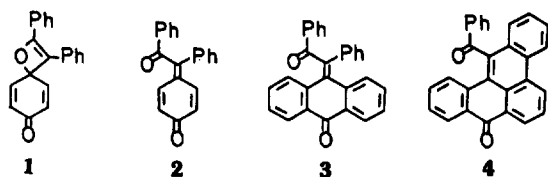
The photochemical addition of *p*-quinones to compounds containing olefinic or acetylenic linkages has been the subject of a number of publications.¹⁻¹¹ Photodimerization of *p*-benzoquinone and some of its methyl derivatives gives either cyclobutanes or spiro-oxetanes depending on the nature of the quinone.¹⁴ The photoaddition of diphenylacetylene to *p*-benzoquinone forms a quinomethane (**2**), through an unstable intermediate, spiro-oxetene(**1**). Tetrachloro-*p*-benzoquinone (chloranil) readily forms a novel photorearrangement product by the photoreaction with some cyclic olefins.¹² Irradiation of the quinonoid compounds and diphenylacetylene in dichloromethane gives the photoproducts, such as **2,3**, or **4**.^{1,3,13,15}

acetylene to anthraquinone forms (**4**) besides (**3**) (ca. 1:1, molar ratio).¹³ Irradiation of a solution of anthraquinone, diphenylacetylene and iodine in dichloromethane gave (**4**) as a major product, and (**3**) as a minor product.¹³ The photoproduct (**3**) readily undergoes dehydrocyclization to (**4**) during the purification by the column chromatography (silica gel).¹³ The photoreaction of anthrone and diphenylacetylene in dichloromethane afforded the photooxidation products such as (**3**), (**4**) and the dimer in air.¹³ We now report that irradiation of conjugated diyne, such as diphenylbutadiyne, and *p*-quinones gives 1:1 photoadducts as the major products.

Experimental

Materials. Dichloromethane, acetonitrile, *n*-hexane, benzene, diethyl ether, ethyl acetate and methanol were purified before use. *p*-Benzoquinone, chloranil, anthraquinone, dicyclopentadiene and diphenylbutadiyne were purchased from Aldrich Chemical Company. The column chromatography was performed by using Kiesel gel (Merck Co., 70-230 mesh). Kiesel gel 60 F254 (Merck Co., silica gel) was used for the thin layer chromatography.

Instruments. Infrared spectra were recorded on a Perkin-Elmer 283B Grating Spectrophotometer in KBr pellets. ¹H-NMR spectra were obtained on a Bruker AC-100 Spectrometer. Mass spectra were obtained on a Jeol GC/MS



Scheme 1

Irradiation of the anthraquinone methide(**3**) causes dehydrocyclization to give the corresponding benzanthrone (**4**).¹⁴

In our previous studies, the photoaddition of diphenyl-